Post-print of: G. Fotyga and K. Nyka, "An algorithm for enhancing macromodeling in finite element analysis of waveguide components," 2017 IEEE MTT-S International Microwave Workshop Series on Advanced Materials and Processes for RF and THz Applications (IMWS-AMP), Pavia, 2017, pp. 1-3, doi: 10.1109/IMWS-AMP.2017.8247351.

# An Algorithm for Enhancing Macromodeling in Finite Element Analysis of Waveguide Components

Grzegorz Fotyga and Krzysztof Nyka, *Member, IEEE*
Faculty of Electronics, Telecommunications and Informatics
Department of Microwave and Antenna Engineering
Gdansk University of Technology
Email: grzfotyg@pg.gda.pl, nyx@eti.pg.gda.pl

***Abstract*—An algorithm for enhancing the finite element method with local model order reduction is presented. The proposed technique can be used in fast frequency domain simulation of waveguide components and resonators. The local reduction process applied to cylindrical subregions is preceded by compression of the number of variables on its boundary. As a result,the finite element large system is converted into a very compact set of linear equations which thus can be solved extremely fast.**

## I. Introduction

Local model order reduction called a macromodeling [1]–[4] is one of the most effective tools used to speed up the finite element method analysis [5], [6]. This paper addresses the issue of the efficiency of macromodel generation which is introduced in the following concise problem statement. Let us assume, that the subspace associated with subregion $\Omega$ (enclosed by the boundary $S$) is subject to local model order reduction. Due to that process the electromagnetic behavior of $\Omega$ with respect to its boundary $S$ is captured by a small dense matrix called a macromodel (see [1] for details). The macromodels are particularly useful when applied in the subregions of the computational domain, which are required to be finely discretized, near small features of the structure causing rapid changes of the electromagnetic field distribution. Two examples of such regions are shown in Fig. 1.

The size of macromodel ($r \times r$) is determined by two factors:

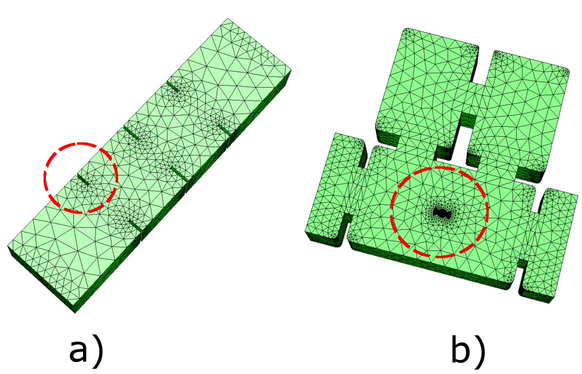


Fig. 1. The two examples of subregions of the computational domain, which are required to be finely discretized, due to the rapid changes of the electromagnetic field distribution.

$$r = 2qn_s, \tag{1}$$

where $q$ is a reduction order and $n_s$ is a number of FEM variables on the boundary $S$, associated with the number of basis functions that approximate the distribution of the electric field on $S$. In practical cases the value of $q$ varies between 5 and 10, whereas the number of variables on $S$ can reach hundreds or even thousands, especially if the three-dimensional FEM formulation with higher-order vector FEM basis functions is employed and dense discretization mesh is required.

In such a case $r$ reaches tens of thousands, which significantly deteriorates the efficiency of macromodeling generation. What is more, if the analysis requires to generate many macromodels, it greatly increases memory usage, since macromodels are stored as full matrices.

Therefore, it is necessary to create a technique, to reduce $r$. Although one should not decrease the value of $q$, since it would affect the accuracy of results, it is possible to limit the value of $n_S$ prior to the local reduction. This can be achieved by an operation in which the distribution of the electric field on the boundary $S$ is approximated by means of the set of $n'_S$ functions, where $n'_S \ll n_S$.

In this paper the technique of compression the number of FEM variables on the cylindrical boundary $S$ is presented. It is based on [7], [8], however in the proposed method the reduced number of functions ($n'_S$) used to approximate the field distribution on $S$ is chosen automatically, which prevents from very time consuming repetitive trial simulations.

## II. Compression of the Number of Variables on the Boundaries

In order to compress the number of FEM variables on $S$, the space of FEM basis functions (defined on $S$) is projected onto a subspace spanned a much smaller the set of $n'_S$ orthogonal functions, expressed as:

$$\mathcal{B}_{\mathcal{S}} = \{\vec{e}_{S1}(x,y,z), \quad \vec{e}_{S2}(x,y,z) \ldots \ \vec{e}_{Sns'}(x,y,z)\}. \tag{2}$$

They are defined analytically, using trigonometric functions and Legendere polynomials, depending on the shape of $S$. The distribution of the electric field on $S$ is defined as follows:

$$\vec{E}_S(x,y,z) \cong \sum_{i=1}^{n'_S} c_i \vec{e}_{Si}(x,y,z). \tag{3}$$

In order to project the FEM space from $S$ onto a subspace defined by (2), one has to represent $\mathcal{B}_S$ as a set of discretized functions spanned by a subspace of FEM basis functions. Note, that $S$ is a surface, therefore only two-dimensional FEM basis functions are used. Each of the functions from (2) can be approximated by the FEM expansion:

$$\vec{e}_{Sk}(x,y,z) \cong \sum_{i=1}^{n_s} e_i \vec{T}_{Si}(x,y,z). \tag{4}$$

where $k \in \{1, 2 \ldots n'_S\}$, $\vec{T}_{Si}(x,y,z)$ are a FEM basis functions, $n_S$ is a number of basis functions defined on $S$ and $e_i$ are expansion coefficients. Next, both sides of (4) are multiplied by $\vec{T}_{Sj}(x,y,z)$, where $j \in \{1, 2, \ldots n_s\}$ and integrated over $S$:

$$\begin{aligned}\sum_{j=1}^{n_s} \int_S \vec{T}_{Sj}(x,y,z) \cdot \vec{e}_{Sk}(x,y,z) dS \cong \\ \sum_{j=1}^{n_s} \sum_{i=1}^{n_s} \int_S \vec{T}_{Sj}(x,y,z) \cdot \vec{T}_{Si}(x,y,z) dS \ e_i.\end{aligned} \tag{5}$$

Note, that the right-hand side of equation (5) can be represented by a FEM mass matrix (denoted as $\mathbf{C}$). Therefore, the above equation can be rewritten as follows:

$$\mathbf{C}_S \mathbf{e}_{Sk} = \mathbf{f}_{Sk}, \tag{6}$$

where vectors $\mathbf{f}_{Sk}$ and $\mathbf{e}_{Sk} \in C^{n_S}$, whereas $\mathbf{C}_S \in C^{n_S \times n_S}$. Each of the elements of $\mathbf{C}_S$ and $\mathbf{f}_{Sk}$ is obtained in the following manner:

$$\begin{aligned}\mathbf{C}_{Sji} &= \int_S \vec{T}_{Sj}(x,y,z) \cdot \vec{T}_{Si}(x,y,z) dS, \\ \mathbf{f}_{Skj} &= \int_S \vec{T}_{Sj}(x,y,z) \cdot \vec{e}_{Sk}(x,y,z) dS.\end{aligned} \tag{7}$$

The integrals in (7) can be solved by means of the Gauss quadrature [5], [6].

Once the system of equations (6) is solved for $k \in \{1, 2 \ldots n'_S\}$, one obtains a discretized form of (2), which is a projection basis of the size $n_S \times n'_S$:

$$\mathbf{B_S} = [\mathbf{e}_{S1}, \ \mathbf{e}_{S2} \ldots \mathbf{e}_{Sns'}]. \tag{8}$$

Subsequently, the appropriate blocks in the original FEM system of equations (which correspond to $\Omega 1$ - outer region, $S$ - boundary and $\Omega$ - subregion subject to local reduction) are project on the subspace spanned by the vectors of $\mathbf{B_S}$:

$$\begin{bmatrix} \mathbf{A}_{\Omega 1} & \mathbf{A}'_1 & 0 \\ \mathbf{A}'^T_1 & \mathbf{A}'_S & \mathbf{A}'_2 \\ 0 & \mathbf{A}'^T_2 & \mathbf{A}_\Omega \end{bmatrix} \cdot \begin{bmatrix} \mathbf{e}_{\Omega 1} \\ \mathbf{e}'_S \\ \mathbf{e}_\Omega \end{bmatrix} = \begin{bmatrix} \mathbf{b} \\ \mathbf{0} \\ \mathbf{0} \end{bmatrix}. \tag{9}$$

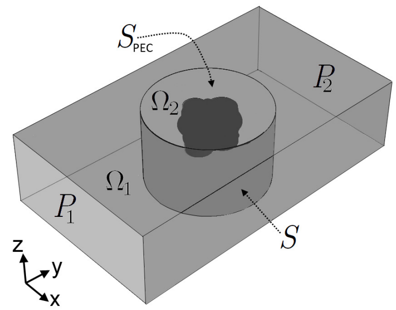


Fig. 2. Waveguide structure bounded by the two ports ($P_1$ and $P_2$), and perfect electric conductor (PEC). The boundary $S$ divides the computational domain into $\Omega_1$ and $\Omega_2$.

where:

$$\begin{aligned}\mathbf{A}'_S &= \mathbf{B}_S^T \mathbf{A}_S \mathbf{B}_S \\ \mathbf{A}'_1 &= \mathbf{A}_1 \mathbf{B}_S \\ \mathbf{A}'_2 &= \mathbf{B}_S^T \mathbf{A}_2 \\ \mathbf{e}_S &\approx \mathbf{B}_S \mathbf{e}'_S.\end{aligned} \tag{10}$$

## III. Cylindrical boundary

The procedure presented in the previous section is now adopted to compress the number of variables on the cylindrical boundary $S$ (Fig. 2).

If the local reduction is planned in subregion $\Omega_2$, a compression of the number of variables has to be performed on the boundary $S$. The distribution of the vectorial electric field on $S$ can be approximated by the series:

$$\begin{aligned}\vec{E}_S(\phi, z) = \vec{i_z} \sum_{m=1}^{L_m} \sum_{k=0}^{L_k} a^{\mathrm{I}}_{mk} \sin(m\phi) \cos(k\frac{z}{h}\pi) + \\ \vec{i_z} \sum_{m=0}^{L_m} \sum_{k=0}^{L_k} a^{\mathrm{II}}_{mk} \cos(m\phi) \cos(k\frac{z}{h}\pi) + \\ \vec{i_\phi} \sum_{m=0}^{L_m} \sum_{k=1}^{L_k} a^{\mathrm{III}}_{mk} \cos(m\phi) \sin(k\frac{z}{h}\pi) + \\ \vec{i_\phi} \sum_{m=1}^{L_m} \sum_{k=1}^{L_k} a^{\mathrm{IV}}_{mk} \sin(m\phi) \sin(k\frac{z}{h}\pi),\end{aligned} \tag{11}$$

where $h$ is the height of a waveguide and $a^{\mathrm{I}}_{mk} \ldots a^{\mathrm{VI}}_{mk}$ are the expansion coefficients. Fig. 3 shows the $\vec{i_z}$ component of the electric field on $S$ for the two example functions from (11). The number of functions $n'_S$ in series (11) is equal to:

$$n'_S = 4L_m L_k + 2L_m + 2L_k + 1. \tag{12}$$

The values of $L_m$ and $L_m$ can be determined by the following formulas:

$$L_m = L = \lfloor \frac{2\pi r \tau f_{max}}{c} \rfloor, \tag{13}$$

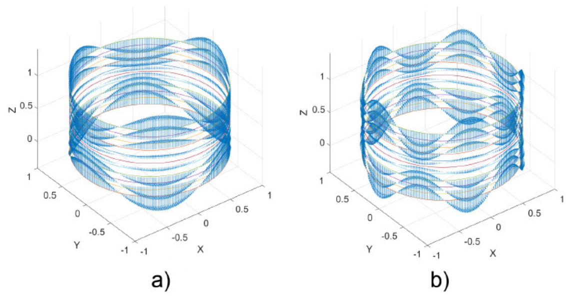


Fig. 3. The $\vec{i_z}$ component of the electric field on $S$ for the two example functions from (11). a) $\vec{E}_S(\phi, z) = \vec{i_z}\cos(3\phi)\cos(\frac{z}{h}\pi)$ b) $\vec{E}_S(\phi, z) = \vec{i_z}\cos(5\phi)\cos(\frac{z}{h}\pi)$

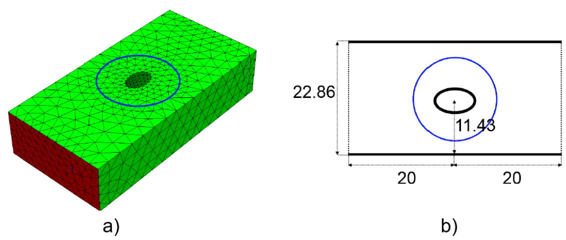


Fig. 4. Dimensions in mm of a waveguide with discontinuity. Height of the discontinuity: 6.16 mm. The length of the axes of the elliptical cross-section: 2 mm and 3 mm.

$$L_k = \lfloor \frac{2h\tau f_{max}}{c} \rfloor, \tag{14}$$

where $f_{max}$ is the max frequency of the analysis, $r$ is the radius of the cylinder, $c$ is the speed of light and $\tau \in \{1, 2, 3 \dots\}$. Although $\tau$ is a heuristic parameter the number of necessary trials is significantly lower than those needed without equations (13) and (14).

In effect of the compression of the variables on $S$, the size of the macromodel is much smaller, comparing to the original one, assuming the same value of $q$:

$$(r' = 2qn'_s) \ll (r = 2qn_s). \tag{15}$$

## IV. Numerical Results

To investigate the accuracy of the proposed method, a simple waveguide with a discontinuity is analysed (see Fig. 4. for details). Firstly, as the reference results, $S$-parameters have been computed by means of a standard FEM formulation in a bandwidth: 12-15 GHz using 38002 FEM global unknowns and 2108 unknowns on the boundary $S$. Next, the proposed technique has been employed, with $r = 8$ mm and $\tau \in \{1, 2, 3\}$, which gives a compression of variables on $S$: $n'_S \in \{15, 55, 119\}$. Fig. 5 shows the error plots of the analysis comparing to the standard FEM formulation, where the error is defined as follows:

$$\begin{aligned} e_{S_{11}}(s) &= 20\log_{10}(|S_{11}(s) - S_{11red}(s)|), \\ e_{S_{21}}(s) &= 20\log_{10}(|S_{21}(s) - S_{21red}(s)|). \end{aligned} \tag{16}$$

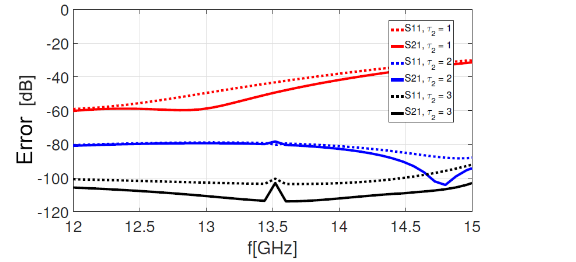


Fig. 5. The error plots of the proposed method comparing to the standard FEM formulation.

It can be seen, that for $\tau = 2$ the error below $-80$ dB, which guarantees that the corresponding $S$-characteristics are almost indistinguishable from each other. In this case the size of macroelement is equal to $275 \times 275$.

## V. Conclusion

A new algorithm for fast frequency simulation of waveguide components and resonators is proposed. It is based on the Finite element method combined with local model order reduction, called macromodeling, and the projection of fields on subdomain boundaries on properly constructed orthogonal basis. In order to determine an optimal size of this basis the analytical formulas are proposed to replace numerous repetitive trial simulations.

## Acknowledgment

This work was partially supported by the TEAM-TECH project entitled EDISOn - Electromagnetic Design of flexIble SensOrs operated within the Foundation for Polish Science TEAM TECH Programme co-financed by the European Regional Development Fund, Operational Programme Smart Growth 20142020, and also by funds from the statutory activities of WETI.

## References

[1] G. Fotyga, M. Rewienski, and M. Mrozowski, "Wideband Macromodels in Finite Element Method," *Microwave and Wireless Components Letters, IEEE*, vol. 25, no. 12, pp. 766–768, 2015.

[2] A. C. Cangellaris, M. Celik, S. Pasha, and L. Zhao, "Electromagnetic model order reduction for system-level modeling," *Microwave Theory and Techniques, IEEE Transactions on*, vol. 47, no. 6, pp. 840–850, 1999.

[3] N. Feng, D. Shuo, Z. Lezhu, and X. Mingyao, "Macro element methods in FEM for 3-D electromagnetic radiation problems," in *Microwave Conference, 2006. APMC 2006. Asia-Pacific*. IEEE, 2006, pp. 1941–1944.

[4] A. C. Cangellaris, "Electromagnetic macro-modeling: An overview of current successes and future opportunities," in *Computational Electromagnetics International Workshop (CEM), 2011*. IEEE, 2011, pp. 1–6.

[5] D. B. Davidson, *Computational Electromagnetics for RF and Microwave Engineering*. Cambridge university press, 2005.

[6] J.-M. Jin, *The Finite Element Method in Electromagnetics*, 3rd ed. New Jersey: John Wiley & Sons, 2014.

[7] G. Fotyga, K. Nyka, and M. Mrozowski, "Multilevel model order reduction with generalized compression of boundaries for 3-D FEM electromagnetic analysis," *Progress In Electromagnetics Research*, vol. 139, pp. 743–759, 2013.

[8] L. Kulas, P. Kowalczyk, and M. Mrozowski, "A novel modal technique for time and frequency domain analysis of waveguide components," *IEEE Microwave and Wireless Components Letters*, vol. 21, no. 1, pp. 7–9, 2011.